Theor Chem Acc (2006) 115: 65–71
DOI 10.1007/s00214-005-0684-6

REGULAR ARTICLE

J.M. Menéndez · I. Martín · A.M. Velasco

Ionization thresholds and positions of avoided crossing of potassium Stark Rydberg states: a Stark-adapted quantum defect orbital treatment

Received: 28 November 2004 / Accepted: 22 June 2005 / Published online: 31 October 2005

Abstract We have calculated the positions of the avoided level crossings between $(n+2)s$, np states and nd, k Stark states in the Rydberg Stark states of the potassium atom with principal quantum number n comprised between 12 and 17. We have also studied the adiabatic electric field ionization thresholds for the above Rydberg states. Both the ionization thresholds and the positions of avoided crossings have been calculated using the recently developed Stark-adapted quantum defect orbital (SQDO) formalism. The presently reported values appear to be in very good agreement with the available theoretical and experimental data.

Keywords Stark effect · Non-hydrogen atoms · Rydberg states · SQDO approach · Stark maps

1 Introduction

Very recently, we have formulated a new approach to determine atomic properties in the presence of an electric field, the Stark quantum defect orbital (SQDO) method [1]. With it, Stark maps and oscillator strengths within the external field have been calculated for the alkali atoms, with the achieved results being in excellent agreement with earlier experimental [2] and theoretical [3] data.

The finite size of the ionic core has several consequences in the properties of the Rydberg states of the alkali atoms. In the absence of an electric field it leads to large quantum defects for the low angular momentum states. In non-zero field, levels which would cross in a hydrogen atom, couple in the alkalis. Below the classical ionization limit this coupling leads to avoided level crossings, and beyond it, to differences in the field ionization of the alkali atoms with respect to that of hydrogen.

In the last few decades, field ionization has been studied both for the intrinsic interest in the process [4] and for its potential applications, such as collision studies [5,6], or as a highly selective detection technique [7,8]. However, the intimately related avoided crossings in atoms other than hydrogen have not been paid much attention in spite of being of interest to both atomic theory [9] and experiment [10]. In experiment, level crossing and anticrossing spectroscopic techniques have been used to investigate properties of atomic Rydberg states such as the extent of the fine structure, Stark and Zeeman shifts, transition probabilities and lifetimes. The anticrossings of Stark levels also play an important role in static field ionization [11,12] and in time-dependent microwave field ionization [13,14]. Theoretically speaking, calculations of the positions of anticrossings are very important to instruct the above experiments and to test the theoretical approaches used to calculate the atomic spectra in electric fields.

There are three commonly employed approaches in this context: the introduction of a spherical core-coupling, as a small perturbation, to hydrogenic parabolic states [15], the diagonalization of a truncated Hamiltonian matrix [3], and a quantum defect theory [16]. But, in practice, only matrix diagonalization has been widely used for stable states. However, because the positions for anticrossings have a sensitive dependence on wavefunctions [17], this kind of theoretical calculation with numerical results is scarcely seen.

Encouraged by the accuracy of our previous study [1], we have now applied the SQDO methodology to the calculation of level-crossing positions as well as field ionization thresholds for the potassium atom in different high-energy (Rydberg) states: the achieved results have been assessed with the help of experimental and theoretical data available in the literature.

The SQDO approach has been described in detail in Menéndez et al. [1]. Thus, we shall only give a brief outline of the present computational method in Sect. 2. In Sect. 3,

J.M. Menéndez · I. Martín (✉) · A.M. Velasco
Departamento de Química Física y Química Inorgánica,
Facultad de Ciencias
Universidad de Valladolid,
47005 Valladolid, Spain
E-mail: imartin@qf.uva.es
Tel.:+34-98-3423272
Fax:+34-98-3423013

field ionization thresholds and positions of avoided crossings will be given and analyzed with the help of comparative data.

2 Computational method

In the presence of an external field and ignoring the relativistic effects, as they have been proven to have very little influence in this context [3], the Hamiltonian for the potassium atom has the following form:

$$H = H_{\text{at}} + Fz, \tag{1}$$

where H_{at} is the field-free atomic Hamiltonian, F is the strength of the applied field, and z is the coordinate of the electron along the direction of the field (the quantization axis). Atomic units are used throughout.

For weak fields, the eigenvalues $|\alpha\rangle$ for the atomic states can be calculated through an expansion of a spherical alkali state basis consisting of the bound eigenstates $|n, l\rangle$ of H_{at}, where $H_{\text{at}}\,|n, l\rangle = E_{n,l}\,|n, l\rangle$ (to simplify the notation, we ignore the magnetic quantum number, m_l, since it is a constant). This expansion may be written as follows:

$$|\alpha\rangle = \sum\nolimits_{n,l} a^{\alpha}_{n,l}\,|n, l\rangle\,, \tag{2}$$

The interaction between the excited electron and the core ion is represented by a model potential that yields accurate quantum defects and satisfies the correct boundary conditions at large and small distances. This potential, as proposed by Simons [18] and Martín and Simons [19], is the starting point of the quantum defect orbital (QDO) formalism [18–20].

A complete description of the QDO method has been presented in previous papers [18–20], for which a relativistic (RQDO) version was later formulated by Martín and Karwowski [21], and succesfully applied to a number of atomic problems [22]. A summary of the most relevant features of the non-relativistic QDO approach [18, 19] follows. It is based on the analytical solution of a one-electron Schrödinger equation, where the model potential includes a screening parameter, which varies with the radial distance, and takes the form:

$$V(r) = \frac{\lambda(\lambda+1) - l(l+1)}{2r^2} - \frac{Z_{\text{net}}}{r}, \tag{3}$$

where Z_{net} is the effective nuclear charge on the outer electron (s). The screening aspects of the model potential are determined by the parameter λ, which is also related to the orbital quantum number, l, through the expression:

$$\lambda = l - \delta_l + c. \tag{4}$$

In Eq. 4, δ_l is the quantum defect of the state being considered, and "c" is an integer chosen, within a narrow range of values, to ensure the normalization of the radial orbital, as well as its correct nodal pattern. The number of radial nodes is equal to $n-l-1-$c, where n is the principal quantum number. Due to the central field symmetry of the model potential, the zero-field wavefunction has the following form:

$$\Psi^{\text{QDO}}_{nlm} = R^{\text{QDO}}_{nl}(r)\,Y_{lm}(\theta, \varphi), \tag{5}$$

where m is the magnetic quantum number. The radial part $R^{\text{QDO}}_{nl}(r)$ of the QDO is the analytical solution of Whittaker's second differential equation [23], and $Y_{l,m}(\theta, \varphi)$ is a spherical harmonic. In the presence of a homogeneous external field, there is a mixing of the states that differ by one unit in their orbital quantum numbers and possess the same magnetic quantum number. The mixings created by the field have been dealt with through different approaches, as mentioned in the Introduction. We have adopted the unperturbed QDO's as an adequate basis to represent the hamiltonian matrix in the presence of the field. Hence, in this procedure, the energy matrix has the following diagonal and off-diagonal terms, respectively:

$$H_{ii} = -\frac{1}{2n^{*2}}, \tag{6}$$

$$H_{ij} = F\delta_{m,m'}\delta_{l,l\pm1}\left\langle R^{\text{QDO}}_{n,l}\,|r|\,R^{\text{QDO}}_{n',l\pm1}\right\rangle \langle Y_{lm}|\cos\theta|Y_{l\pm1m}\rangle\,, \tag{7}$$

where $n^* = n - \delta_l$ is the effective quantum number.

At this point, it is important to notice that all the integrals involved in the hamiltonian diagonalization process, written in terms of the QDO's, are closed-form analytical expressions. This is, in our view, a particular advantage of our procedure from a computational point of view, as all calculations are free from numerical errors and convergence problems.

Another important consideration to our approach is that the off-diagonal elements of r, $\left\langle R^{\text{QDO}}_{n,l}\,|r|\,R^{\text{QDO}}_{n',l\pm1}\right\rangle$ decrease rapidly as the energy difference between the involved states increases. Thus, only those states that are local in energy need be included in the matrix diagonalization process to obtain eigenvalues and eigenvectors in a particular energy region. This ensures a finite character for the basis set, together with a conservation of the analyticity of the original QDO approach.

After the hamiltonian diagonalization, each of the eigenvectors, to which we shall refer as SQDOs, is a linear combination of unperturbed QDO's, as expressed by Eq. 2. In more detail,

$$\left|\Psi^{\text{SQDO}}\right\rangle = \sum_{n}\sum_{l=|m|}^{n-1} U^{n_1,n_2}_{n,l}(F)\left|\Psi^{\text{QDO}}_{nlm}\right\rangle, \tag{8}$$

where $U^{n_1 n_2}_{n,l}(F)$ are the elements of the field-dependent unitary transformation matrix that projects the Stark states onto the corresponding unperturbed states. The former are characterized by the parabolic quantum numbers n_1, n_2 (the numbers n_1 and n_2 take on values comprised between 0 and $n-1$, and are related to the principal quantum number in the form, $n = n_1 + n_2 + |m| + 1$).

3 Results and discussion

3.1 Position of anticrossings

Figure 1 depicts the presently found crossing positions for the $|m_l| = 0, 1$ states of potassium. A_0 and B_0 indicate, respectively, the positions of the avoided crossings between

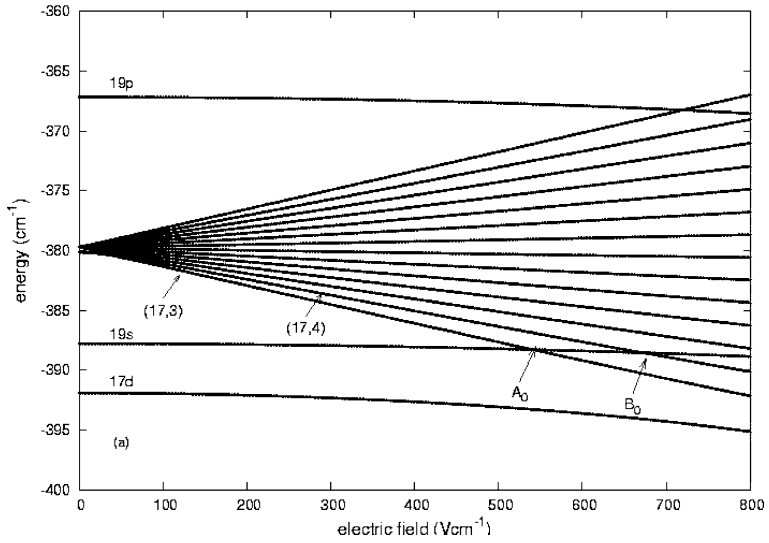

Fig. 1 SQDO positions of the level crossings of potassium in the vicinity of $n = 17$, $m_l = 0$. A_0 and B_0 indicate, respectively, the crossing locations of the (17, 3) and (17, 4) Stark states with the 19s state (for notation see Sect. 3.1)

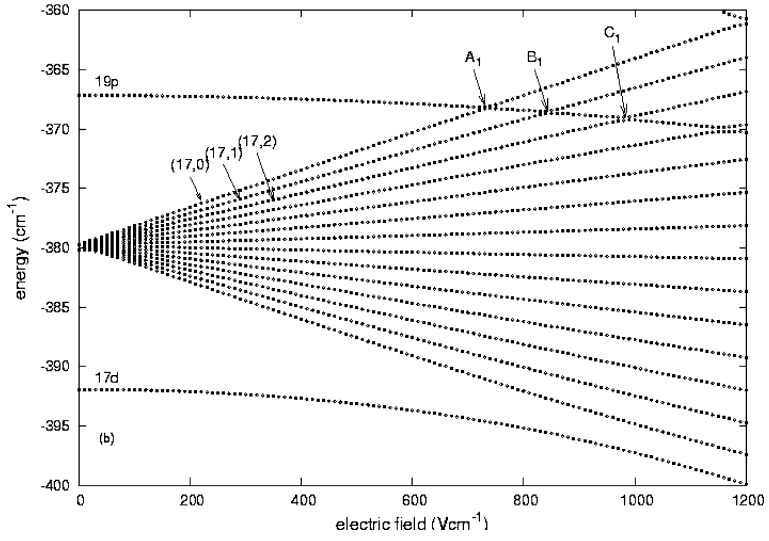

Fig. 2 SQDO positions of the level crossings of potassium in the vicinity of $n = 17$, $m_l = 1$. A_1, B_1 and C_1 indicate, respectively, the crossing locations of the (17, 0), (17, 1) and (17, 2) Stark states with the 19p state

the 19s unperturbed state and the (17, 3) and (17, 4) Stark states. The quantum numbers in the (n_F, n_1) notation here employed for the Stark states are defined in the form, $n_F = n - \mathrm{Int}(\delta_l)$ and $n_1 = n_F - n_2 - |m_l| - 1$, respectively. $\mathrm{Int}(\delta_l)$ is the integer nearest to the rounded value of δ_l, and n_1, n_2 are parabolic quantum numbers. Similarly, in Fig. 2, where the (n_F, n_2) notation is used. A_1, B_1 and C_1 indicate the positions of the crossings between the 19p state and the (17, 1), (17, 2) and (17, 3) Stark states, respectively.

The present calculations of avoided crossing positions have been extended to other s and p states. Accordingly, in Table 1, the locations of the avoided crossings, denoted as A_0 and B_0 in Fig. 1, for the Stark states within the range $n = 13-17$, i.e., 15s to 19s unperturbed states, are displayed. In an analogous manner, the crossing locations A_1, B_1 and C_1 of Fig. 2 have now been collected for the p state-range n = 12–17, i.e., the states comprised between the unperturbed 14p–19p states in Table 2, where the theoretical data reported by Stoneman and Gallagher [10] and Li et al. [17], as well as the measurements by Stoneman et al. [9], have also been included. Of the two mentioned theoretical calculations, i.e., those of Stoneman and Gallagher [10], followed the methodology proposed by Zimmerman et al. [3], where the radial component of the basis functions is a product of generalized Coulomb functions with non-integral n quantum numbers. The radial integrals were numerically determined by using a generic central symmetric potential. Li et al. [17] employed the solutions of a model potential Hamiltonian developed by He et al. [24] as basis functions for the Stark Hamiltonian matrix.

Table 1 Theoretical and observed positions for s-state anticrossings (in V cm^{-1})

s state	$n_1 = 3, \|m_l\| = 0$				$n_1 = 4, \|m_l\| = 0$		
	SQDO[a]	Expt.[b]	Theor.[c]	Theor.[d]	SQDO[a]	Expt.[b]	Theor.[c]
15s	2312.8				3301.4		
16s	1542.2				2084.0		
17s	1061.8				1381.3		
18s	751.4	752.7(8)	752.5	753.80	949.8		955.9
19s	545.6	545.7(8)	545.5	546.40	675.2	674.0(4)	676.5

[a]SQDO this work.
[b]Stoneman et al. [9]
[c]Li et al. [17]
[d]Stoneman and Gallagher [10]

Table 2 Theoretical and observed positions for p-state anticrossings (in Vcm^{-1})

p state	$n_2 = 0, \|m_l\| = 1$			$n_2 = 1, \|m_l\| = 1$		$n_2 = 2, \|m_l\| = 1$	
	SQDO[a]	Expt.[b]	Theor.[c]	SQDO[a]	Theor.[c]	SQDO[a]	Theor.[c]
14p	4434.2			5473.7		6973.7	
15p	2934.8			3565.2		4391.3	
16p	2000.0			2386.4		2924.2	
17p	1399.7			1652.4		1966.7	
18p	1000.0			1168.4		1389.5	
19p	731.6	737.7(13)	733.1	844.7	844.6	986.8	984.4

[a]SQDO this work
[b]Stoneman et al. [9]
[c]Li et al. [17]

As it can be noticed by inspection of Tables 1 and 2, our present results are in rather good accord with the observed values. With the purpose of analyzing the trend followed by the crossing positions, we have plotted, in Fig. 3, the log of the field crossing locations A_0 and B_0 versus the log of the effective quantum number of the state. The experimentally-found crossing positions, A_0 and B_0, have been represented by stars ($*$), and the corresponding SQDO values are indicated by solid circles ($\bullet$). The present SQDO points appear to be superimposed to the measurements, whenever these are available, or, otherwise, they closely follow the trend established by experiment (Fig. 3).

In a similar manner, the n_F p (n_F, 1), (n_F, 2) y (n_F, 3) crossings, denoted as A_1, B_1 and C_1, respectively, are displayed in Fig. 4. Again, the trend exhibited by the SQDO crossing points is in rather good accord with that of the measurements. In all cases (Figs. 3, 4), a linear trend is observed. This suggests a dependence of the crossing locations on the effective quantum number that, according to the logarithmic expressions consistent with the plots in Figs. 3 and 4 $\log(F) = \log(A) + x\log(n^*)$, may be expressed in the following form,

$$F = A(n^*)^x. \tag{9}$$

Given that, for the hydrogen atom, the energy difference between two adjacent states is $1/n^3$ and that the energy difference between the highest Stark state belonging to an n-level and the lowest Stark state of the $(n+1)$-manifold, is equal to $3n^2F$, first-order Perturbation Theory [25] leads to the following relationship between the n-value and the field strength for the first crossing position:

$$F = \frac{1}{3}n^{-5}. \tag{10}$$

Consequently, as a first approximation, a value of $x \approx -5.0$ in Eq. 9 might be assigned to potassium. A least-square fitting of the data plotted in Figs. 3 and 4 yields values of x, equal to -5.3 and -5.8, for A_0 and B_0 respectively, and to -5.2, -5.4 and -5.7, for A_1, B_1 and C_1, respectively. One can also notice that as n_i increases from $i = 1$ to $i = 2$, the exponent becomes more negative and the crossings shift towards greater field strengths.

3.2 Field ionization

The potential function for a single electron subject to both a Coulomb field and an external field, F, applied along the z axis, is:

$$V_F(r) = -\frac{1}{r} + Fz. \tag{11}$$

This potential exhibits a saddle point on the z axis at the value $V_{sp} = -2\sqrt{F}$. In any state, an atom is ionized if its energy is higher than V_{sp}. Thus, bound states are allowed only for levels that satisfy:

$$W \leq -2\sqrt{F}. \tag{12}$$

However, Eq. 12 is only valid for states with zero angular momentum [26]. For an electron with non-zero magnetic

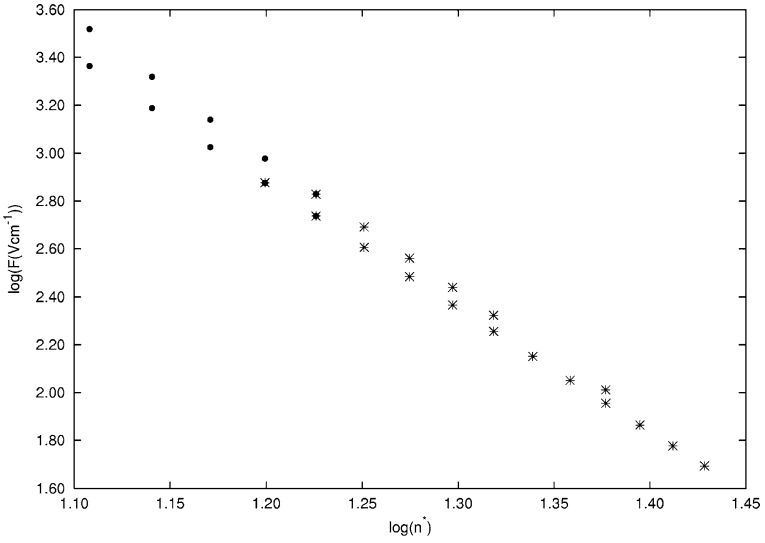

Fig. 3 Log-log plot of the anticrossing field locations for the $15s$ to $19s$ states versus the effective quantum number. Present SQDO calculations are represented by *solid circles*. Experimental results are indicated by *stars*

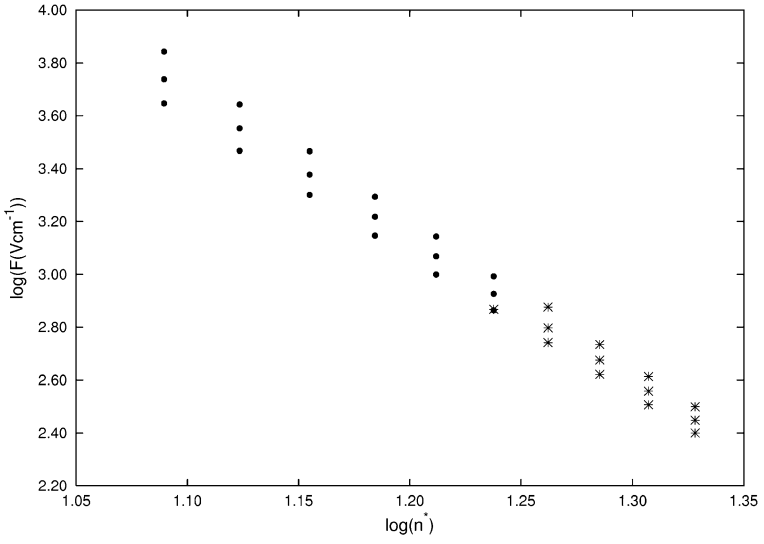

Fig. 4 Log-log plot of the anticrossing field locations for the $19p$ state versus the effective quantum number. Present SQDO calculations are represented by *solid circles*. Experimental results are indicated by *stars*

quantum number, m_l, part of its kinetic energy is used in generating a momentum perpendicular to direction of the field. However, according to Cooke et al. [27], this energy cannot be used by the electron to escape the atom, and, consequently, a higher field is neccessary to ionize the atom. When $|m_l|$ happens to be much lower than n, the saddle point occurs at a value of the potential given by $V_{\rm sp} = -2\sqrt{F} + |m|\,F^{3/4} + \frac{3}{16}m^2F$, and the region of stability is now the following:

$$W \leq -2\sqrt{F} + |m|\,F^{3/4} + \frac{3}{16}m^2F. \tag{13}$$

As mentioned in the Introduction, the Stark map of a non-hydrogen atom is not simple because of the finite size of the core. Accordingly, care must be taken in establishing the passage from low field to ionizing field values. It is well known that the dynamics at each crossing are very well described by the Landau–Zener theory [28], and the probability that a given crossing is traversed adiabatically (i.e., that the system undergoes a transition from a Stark state i to another state j) or diabatically (i.e., the system remains in the same Stark state i) depends on the matrix element that couples both states and on the electric field slew rate. In this work we have considered that all the crossings are traversed adiabatically, so that we can compare our results with the available experimental data.

The ns and np states of potassium have large quantum defects ($\delta_s = 2.178$, $\delta_p = 1.712$) and, as the field increases, they initially encounter states belonging to neighboring Stark manifolds of different n. In contrast, the nd states have a small quantum defect ($\delta_d = 0.267$), and the Stark states that they

Table 3 Theoretical and observed field ionization thresholds in $KVcm^{-1}$ for states with $|m_l| = 0, 1$

State	$\|m_l\| = 0$	$\|m_l\| = 1$	$\|m_l\| = 0, 1$
	SQDO[a]	SQDO[a]	Expt.[b]
14*s*	19.17		
15*s*	13.64		
16*s*	10.09		
17*s*	7.74		7.46, 7.58, 7.73, 7.88
18*s*	5.76		5.65, 5.83, 6.00, 6.12
19*s*	4.60		4.42, 4.55
14*p*	14.14	14.61	
15*p*	10.62	10.99	
16*p*	7.93	8.27	
17*p*	6.15	6.34	
18*p*	4.67	4.92	4.54, 4.76, 4.91
19*p*	3.73	3.86	3.62, 3.86
12*d*	19.80	20.66	
13*d*	14.17	14.66	
14*d*	10.31	10.67	
15*d*	7.85	8.13	7.56, 7.81
16*d*	6.08	6.17	5.80, 5.96, 6.14
17*d*	4.69	4.85	4.60, 4.73, 4.91
18*d*	3.69		3.61, 3.71

[a]Present calculations
[b]Gallagher et al. [31]

Table 4 Theoretical and observed field ionization thresholds in $KVcm^{-1}$ for states with $|m_l| = 2$

State	$\|m_l\| = 2$	
	SQDO[a]	Expt.[b]
12*d*	21.46	
13*d*	15.63	
14*d*	11.23	
15*d*	8.48	8.57 ± 0.26
16*d*	6.46	6.47 ± 0.19
17*d*	5.02	5.04 ± 0.15

[a]Present calculations
[b]Gallagher et al. [31]

encounter first have the same n value. Given that coupling is strongest between states belonging to the same n manifold, marked differences in behavior at the ensuing avoided crossings happen. As a d state approaches its neighboring manifold, strong mixing leads to the appearance of broad avoided crossings. The s and p states couple less strongly to their neighboring Stark states, resulting in a series of narrow avoided crossings and, consequently, the adiabatically connected states preserve much more of their initial character. This leads to the fact that from the first avoided crossing to the point where field ionization occurs, a smooth trajectory cannot be considered even for states with $m_l = 0$ as it happened in Sodium [29,30]. As a consequence, ionization thresholds are determined by following the trajectory of the different states until they reach the classical limit given by Eq. 13, in the corresponding SQDO Stark maps, assuming that all the crossings occur adiabatically.

In contrast to the behavior found in the sodium atom [5], the experimental avoided crossing locations for the s, p and d states with $m_l = 0$ and $m_l = 1$ of potassium exhibit certain multiplicity, as shown in Table 3. According to Gallagher et al. [31], this feature may be attributed to the existence of spin-orbit coupling in potassium which, unlike in Na, leads to a splitting of levels. This splitting is partly adiabatic in the passage from low fields (where m_j is well defined), to intermediate fields (where m_l and m_s are good quantum numbers), giving rise to a number of different pathways towards ionization.

As a further evidence of the above feature, it has been experimentally [31] determined that atoms follow adiabatic paths towards ionization. Thus, partially diabatic traversals of intermediate-field crossings are not the source of the multiple ionization thresholds.

The partly adiabatic passage, and its consequences on the goodness of m_j, prevents a distinction between the ionization thresholds that correspond, respectively, to the $m_l = 0$ and $m_l = 1$ states. From the point of view of the theory, establishing such a distinction would be a difficult and complex task, given the large number of combinations that are possible. Nevertheless, a comparison of the present results (Table 3), obtained on the grounds of a field ionization that is totally adiabatic, with the experimental values of Gallagher et al. [31], reveals that, in all the cases considered, the latter include a value that is very close in magnitude to the ones we have calculated. That is, we might conclude that, accepting the existence of a variety of pathways to ionization, one that corresponds to an adiabatic ionization will always be found. Moreover, for certain states, such as $18d$ and $19p$, adiabatic ionization appears to be the only possibility.

For the states of potassium characterized by $m_l = 2$, the present SQDO ionization thresholds are compared with the measurements by Gallagher et al. [31] in Table 4. The lack of multiplicity in the experimental thresholds allows us a direct comparison with our calculated values, which reveals an excellent accord with the experiment [31]. This suggests, once more, the adequacy of the SQDO formalism to the analysis of field ionization.

4 Conclusions

Positions of avoided crossings and field ionization thresholds have been determined for the Rydberg states of the potassium atom. The SQDO procedure, which involves a Hamiltonian diagonalization [1] with quantum defect orbitals [18] as basis functions, has yielded results that agree rather well with experimental data. This fact, added to our previous studies [1], suggests the SQDO method to be a useful tool for studying the behavior of atoms in the presence of an external electric field. This approach also includes the capability of identifiying different ionization pathways that cannot be experimentally resolved.

The present calculations, however, ignore the spin-orbit (SO) interaction. In this sense, the orbital magnetic quantum number is taken as an approximately good quantum number.

This may be justified on the grounds that the SO splitting in potassium is small. Furthemore, the calculation by Stoneman et al. [9] showed that m_l is indeed an approximately good quantum number. Also, Gallagher et al. [31] came to the conclusion that the effect of spin-orbit coupling in potassium is just a blurring in the resolved $|m_l|$ thresholds, with no consequences on the gross features of its field ionization behavior. For these reasons, one would expect that the errors derived from ignoring the SO interaction should be small. Nonetheless, it is our intention, in the near future, to include fine structure and other relevant relativistic effects in our methodology by adopting, as a starting point, the RQDO formulation [21], where the SO and other relevant relativistic features are accounted for. A field-perturbed matrix diagonalization with RQDOs as basis functions may be expected to deal properly with the influence of the SO splitting, and other relativistic effects, on the anticrossings in the atom of potassium, as well as on heavy and highly ionized atoms.

Acknowledgements This work has been supported by the D.G.I. of the Spanish Ministry for Science and Technology and by European FEDER funds within Projects No. BQU2001-2935-C02 and No. CTQ2004-07768-C02-02. J. M. Menéndez also wishes to acknowledge a research grant awarded by the first institution.

References

1. Menéndez J-M, Martín I, Velasco AM (2003) J Chem Phys 24:12926
2. Littman MG, Zimmerman ML, Ducas TW, Freeman RR, Kleppner D (1976) Phys Rev Lett 36:788
3. Zimmerman ML, Littman MG, Kash MM, Kleppner D (1979) Phys Rev A 20:2251
4. Robicheaux F (1997) Phys Rev A 56:R3358
5. Gallagher TF, Cooke WE, Edelstein SA (1978) Phys Rev A 17:904
6. Smith KA, Kellert FG, Rundel RD, Dunning FB, Stebbings RF (1970) Phys Rev Lett 40:1362
7. Ducas TW, Littman MG, Freeman RR, Kleppner D (1975) Phys Rev Lett 35:366
8. Gigosos MA, Mar S, Pérez C, de la Rosa I (1994) Phys Rev E 49:575
9. Stoneman RC, Janik G, Gallagher TF (1986) Phys Rev A 34:2952
10. Stoneman RC, Gallagher TF (1985) Phys Rev Lett 55:2567
11. Rubmark R, Kash MM, Littman MG, Kleppner D (1981) Phys Rev A 23:3107
12. Gallagher TF, Humphrey LM, Cooke WE, Hill RM, Edelstein SA (1977) Phys Rev A 16:1098
13. Van Linden Van den Heuvel HB, Vachru R, Tran NH, Gallagher TF (1984) Phys Rev Lett 53:1901
14. Stokely CL, Lancaster JC, Dunning FB, Arbo DG, Reinhold CO, Burgdöfer J (2003) Phys Rev A 67:013403
15. Komarov IV, Grozdanov TP, Janev RK (1980) J Phys B: At Mol Phys Opt Phys 13:573
16. Harmin DA (1982) Phys Rev A 26:2656
17. Li Y, Liu W, Li B (1996) J Phys B: At Mol Opt Phys 29:1433
18. Simons G (1984) J Chem Phys 60:645
19. Martín I, Simons G (1985) J Chem Phys 62:4799
20. Martín I, Simons G (1976) Mol Phys 32:1017
21. Martín I, Karwoski J (1991) J Phys B: At Mol Opt Phys 24:1539
22. Martín I, Velasco AM, Lavín C (2000) In: MCWeeny R. et al., (eds.) Progress in theoretical chemistry, Kluwer Academic Publishers, Dordrecht
23. Abramowitz M, Stegun IA (1970) Handbook of mathematical functions, Dover Publications, New York
24. He X, Li B, Chen A, Zhang C (1990) J Phys B: At Mol Phys Opt Phys 23:661
25. Silverstone HJ (1978) Phys Rev A 18:1853
26. Gallagher TF (1994) Rydberg atoms. Cambridge University Press, London
27. Cooke WE, Gallagher TF (1978) Phys Rev A 17:1226
28. Rubbmark JR, Kash MM, Littman MG, Kleppner D, (1981) Phys Rev A 23:3107
29. Jeys TH, Foltz GW, Beiting EJ, Kellert FG, Dunning FB, Stebbings RF (1980) Phys Rev Lett 44:390
30. Merkt F (1997) Annu Rev Phys Chem 48:675
31. Gallagher TF, Cooke WE (1979) Phys Rev A 19:694